Abdominal Radiology (2019) 44:1481–1492
https://doi.org/10.1007/s00261-018-1857-9

Estimation of split renal function using different volumetric methods: inter- and intraindividual comparison between MRI and CT

Florian Siedek[1] · Stefan Haneder[1] · Jonas Dörner[1] · John N. Morelli[2] · Seung-Hun Chon[3] · David Maintz[1] · Christian Houbois[1]

Published online: 1 December 2018

Abstract

Purpose This study aims to determine whether contrast-enhanced (CE)-magnetic resonance imaging (MRI) is comparable to CE-computed tomography (CT) for estimation of split renal function (SRF). For this purpose, two different kidney volumetry methods, the renal cortex volumetry (RCV) and modified ellipsoid volume (MELV), are compared for both acquisition types (CT vs. MRI) with regard to accuracy and reliability, subsequently referred to as RCV_{CT}/RCV_{MRI} and $MELV_{CT}$/$MELV_{MRI}$.

Methods This retrospective study included 29 patients (18 men and 11 women; mean age 62.8 ± 12.4 years) who underwent CE-MRI and CE-CT of the abdomen within a period of 3 months. Two independent readers (R1/R2) performed RCV and MELV in all datasets with corresponding semiautomated software tools. RCV was performed with datasets in the arterial phase and MELV in the venous phase. Statistics were calculated using one-way ANOVA, two-tailed Student's *t* test, Pearsońs correlation, and Bland–Altman plots with $p \leq 0.05$ being considered statistically significant.

Results In all datasets, SRF was almost identical for both volumetry methods with a mean difference of < 1%. Bland–Altman analysis comparing RCV in CT and MRI showed very good agreement for R1/R2. Interreader agreement was strong for RCV_{CT} and good for RCV_{MRI} ($r = 0.89$; $r = 0.69$). $MELV_{CT/MRI}$ interreader agreement was only moderate ($r = 0.54$; $r = 0.50$) with a high range of values. Intrareader agreement was excellent for all measurements, except $MELV_{MRI}$ which showed a high mean bias and range of values (RCV_{CT}: $r = 0.93$, RCV_{MRI}: $r = 0.98$, $MELV_{CT}$: $r = 0.89$, $MELV_{MRI}$: $r = 0.54$).

Conclusion Renal volumetric estimates of SRF are almost as accurate and reliable with CE-MRI as with CE-CT using RCV method. In distinction, the calculation of SRF using MELV was inferior to RCV with respect to accuracy and reliability. Thus, RCV method is recommended to estimate SRF, primarily using CT datasets. However, RCV with MRI datasets for kidney volumetry allows for comparable accuracy and reliability while sparing patients and healthy donors of unnecessary radiation exposure.

Keywords Renal cortex volumetry · Modified ellipsoid volume · Split renal function · Kidney · Living kidney donation

Abbreviations

CE	Contrast-enhanced
CI	Confidence interval
eGFR	Estimated glomerular filtration rate calculated with the "chronic kidney disease epidemiology collaboration" (CKD-EPI) formula
LKD	Living kidney donation

✉ Christian Houbois
christian.houbois@uk-koeln.de

[1] Institute of Diagnostic and Interventional Radiology, University Hospital Cologne, Kerpener Str. 62, 50937 Cologne, Germany

[2] St. John's Medical Center, 1923 South Utica Ave, Tulsa, OK 74104, USA

[3] General, Visceral, and Cancer Surgery, University Hospital Cologne, Cologne, Germany

LoA	Limits of agreement
MELV	Modified ellipsoid volume
$MELV_{CT}$	MELV measurements performed using venous-phase images acquired with CE-CT
$MELV_{MRI}$	MELV measurements performed using venous-phase images acquired with CE-MRI
MIP	Maximum intensity projection
NASCET	The North American Symptomatic Carotid Endarterectomy Trial
RCV	Renal cortex volumetry
RCV_{CT}	RCV measurements performed using arterial-phase images acquired with CE-CT
RCV_{MRI}	RCV measurements performed using arterial-phase images acquired with CE-MRI
ROI	Region of interest
SRF	Split renal function
TKV	Total kidney volume

Introduction

Living kidney donation (LKD) is one treatment option for patients with end-stage renal disease [1–3]. In LKD, the safety of the healthy kidney donor is crucial. Therefore, the kidney donor should always retain the higher functioning kidney as potential complications could arise if its function subsequently becomes impaired (e.g., due to long-standing hypertension). To aid in this determination, both renal anatomic and functional information is required. The performance distribution of each kidney is expressed by the so-called split renal function (SRF).

For the last few decades, the gold standard for determination of SRF has been the dynamic scintirenography, usually using the tracer ^{99m}Tc-mercaptoacetyltriglycine (^{99m}Tc-MAG3-scintigraphy), or alternatively the tracer ^{99m}Tc-diethylene-triamine-pentaacetic acid (^{99m}Tc-DTPA-scintigraphy). However, due to intrinsic limitations of these methods, the adoptions of these techniques have been increasingly questioned. Besides renal scintigraphy, several volumetric methods for determining SRF based on cross-sectional imaging are available and have been increasingly incorporated into the clinical routine [4–7]. For these volumetric methods, most commonly preoperative computed tomography (CT) datasets are used. Current software solutions facilitate automatic or semiautomatic volumetry of the kidneys in these CT datasets. Compared to manual segmentation, these software tools are time saving and increase the reproducibility of SRF measurements [8]. Based on the former literature [5, 6], the most prevalent and promising methods are the renal cortex volumetry (RCV) and modified ellipsoid volume (MELV). Wahba et al. [5] described that estimated SRF evaluated with these techniques is significantly correlating with graft function after kidney transplantation. Also, Soga et al. [6] described a high correlation of estimated SRF evaluated with above techniques with nuclear renography providing accurate information regarding determination of the dominant kidney.

RCV aims to quantify volume of the renal cortex as a surrogate parameter for the "functional part" of the kidney [9]. For RCV, contrast-enhanced (CE) CT-images in the arterial phase are typically used. The early enhancement of the renal cortex leads to improved contrast between the renal cortex and medulla allowing for superior cortical differentiation. The renal cortex can be demarcated accurately, and the cortical volume can be calculated for each kidney separately. In contrast, MELV is a simpler and faster method to assess the complete renal volume. For MELV, venous-phase images of each kidney must be reformatted in 3 cm maximum intensity projections (MIP). A MIP reconstruction oriented along the true long axis of each kidney theoretically simplifies the determination of the maximum renal length and width on para-coronal images and the determination of thickness on para-sagittal images [6]. Width and thickness are measured at the level of the hilum. Both RCV and MELV have advantages and disadvantages regarding interreader variability, time requirements, and complexity of the method.

In the current preoperative evaluation before living kidney donation, cross-sectional imaging is a cornerstone to evaluate the donor's anatomy before surgery. Most frequently, a multi-phase CE-CT examination of the abdomen is performed. However, as living kidney donors are more commonly healthy individuals, an alternative for preoperative imaging without radiation exposure would be desirable. In recent years, further technical improvements in magnetic resonance imaging (MRI) in terms of increased field strengths, stronger gradient fields, and pulse sequences have resulted in higher spatial and temporal resolutions, widening the diagnostic spectrum for MRI. Among other examples, high-quality MR-angiography of the abdominal vessels is diagnostically equivalent to CT angiography [10, 11]. Furthermore, volumetric assessments, e.g., of the liver, show comparable results between MRI and CT datasets [12–14].

To date, comparisons between the two main methods for renal volumetry—RCV and MELV—have been published, but only using CT datasets. No direct, intraindividual comparisons between CT and MRI are available in the literature. Therefore, the aims of this study are to compare (1) RCV between CT and MRI; (2) MELV between CT and MRI; (3) SRF determined with RCV and MELV on CT and MRI; and (4) Inter- and intrareader agreements for both RCV and MELV on CT and MRI.

Materials and methods

Study population

The local institutional review board approved this retrospective study and waived the requirement for informed consent. One radiologist (C.H.) retrospectively searched the local radiology information system (RIS) from 01/2016 to 05/2017 to identify all patients who had undergone a biphasic CE-CT as well as a CE-MRI of the abdomen within 3 months of each other. All examinations were clinically indicated and primarily represented baseline and follow-up studies for oncologic assessment of various abdominal cancer types such as HCC, pancreas carcinoma and gastro-intestinal tumors as well as other nonabdominal diseases with the purpose to rule out abdominal metastases. Only data from patients over 18 years old were included in this study. Exclusion criteria were renal pathologies such as tumor, prior nephrectomy, and renal artery stenosis (> 10% analog to the NASCET criteria). The order of the imaging examinations did not serve as inclusion criterion. Additional clinical data such as creatinine level (Cr) and glomerular filtration rate (eGFR) were registered from the local clinical information system. eGFR was calculated with the "Chronic Kidney Disease Epidemiology Collaboration" (CKD-EPI) formula.

Computed tomography

All CT examinations were conducted with a state-of-the art 128 slice CT scanner (IQon or iCT 256; Philips Healthcare, Best, The Netherlands) in a supine, head first position. Relevant scan parameters were the same with a tube potential of 120 kV and an activated standard clinical dose modulation algorithm (DoseRight 3D-DOM or Z-DOM; Philips Healthcare, Best, The Netherlands). In all patients, 100–120 cc nonionic, iodinated contrast agent (Accupaque 350 mg/mL, GE Healthcare; Little Chalfort, UK) was administered intravenously. Contrast was administered with an automated injector (MEDRAD, Bayer Healthcare, Berlin, Germany) at a mean flow rate of approximately 3.5 cc/s in a peripheral vein followed by a 30 cc saline flush. For contrast timing, a bolus tracking technique was used. To obtain arterial-phase images, the scan began automatically 16 s after reaching the threshold value of 150 Hounsfield units in a circular region-of-interest (ROI) placed within the lumen of the descending aorta. For venous-phase images, the scan was delayed by 50 s after the threshold trigger was met. The arterial- and venous-phase datasets were reconstructed on both scanners with a slice thickness of 2 mm, an iterative reconstruction algorithm with a denoising level of 3 (iDose, Philips Healthcare, Best, The Netherlands), and the same B kernel. Additional scan parameters were as follows: matrix—512 × 512 pixels; section increment—1 mm; mean mAs—146; $CTDI_{vol}$—11.5 ± 4.9 mGy; mean dose-length-product (DLP)—316 ± 151.9 mGy * cm.

Magnetic resonance imaging

All MRI examinations were performed on a clinical, whole-body 3 Tesla MR-scanner (Ingenia, Philips Healthcare, Best, The Netherlands) in a supine, head first position. The MR-scanner was equipped with a standard body-matrix coil and built-in spine-matrix coil for signal reception. Intravenous contrast material was administered as a single dose adapted to the patients' bodyweight with 0.1 mmol/kg BW gadolinium (Gadoterate meglumine [Dotarem], Guerbet, France). An automated injection system (MEDRAD, Bayer Healthcare, Berlin, Germany) was used with a mean flow rate of approximately 2.0 cc/s in the peripheral veins followed by a 30 cc saline flush.

All patients underwent a standard protocol for examination of the upper abdomen. This included dynamic T1-weighted, contrast-enhanced gradient echo sequences with spectral fat suppression for image acquisition at fixed time intervals after administration of contrast agent (0–20 s—1 min–2 min–4 min post injection). Each sequence was performed with breath-hold technique. The relevant sequence parameters were time of repetition—3.1 ms; time of echo—1.49 ms; field-of-view—375 × 354 mm^2; matrix—268 (frequency encoding steps) × 167 (phase encoding steps); reconstructed slice thickness—2 mm; spatial resolution—1 × 1 × 2 mm^3; flip angle—10°.

CT/MRI image analysis

To estimate the cortex/medulla ratios between renal cortex and renal medulla on both imaging modalities, which is crucial for the assessment of the RCV, one board-certified radiologist (S.H.) placed in each anatomic structure one circular ROI on each side at the level of the hilum. ROI measurements were averaged for each patient.

One board-certified radiologist (C.H.) with 9 years work experience and one resident (F.S.) with 5 years work experience analyzed all CT and MRI datasets in a blinded and independent manner after a consensus training session with five patient datasets. The RCV measurements were performed using the arterial-phase images acquired with CE-CT (referred to as RCV_{CT}) and CE-MRI (referred to as RCV_{MRI}) utilizing the semiautomatic volumetric tool included in the Intellispace Platform (ISP 9.0, Philips

Healthcare, Best, The Netherlands). This tool is based on a three-dimensional, region-growing algorithm with preset threshold values. The CT and MRI datasets are automatically resampled and shown in three dimensions. The readers set the point of origin in all three dimensions in the renal cortex and manually adjusted the tool-based recognition of the cortex in all planes. Structures such as renal cysts were manually excluded from volumetry if not automatically detected by the software. Finally, the software calculated the renal volume for each kidney separately. An example image is provided in Fig. 1.

For the MELV method, the venous phase of the CE-CT (referred to as $MELV_{CT}$) and CE-MRI (referred to as $MELV_{MRI}$) datasets were used. Each kidney was reformatted in parasagittal, paracoronal, and paraxial planes and oriented along its true long axis in each orientation using the 3D tool of a clinical DICOM viewer (IMPAX EE, AGFA Healthcare, Mortsel, Belgium). This 3D tool allows generation of maximum intensity projections (MIP) with a thickness of 3 cm in the individually adjusted orientations. Finally, length and width were measured on paracoronal MIPs and thickness in the parasagittal plane. Total kidney volume was calculated using the modified ellipsoid formula: length $\times$ width $\times$ thickness $\times$ $(\frac{\pi}{6})$. An example image is given in Fig. 1.

For the analysis of Intrareader agreement, ten patients were randomly chosen from the study population using an online randomizer (www.randomizer.org). One reader (F.S.) analyzed RCV as well as MELV in a second reading session one month after the first.

Statistical analysis

Statistical analyses were performed by J.D. using Prism Statistics (Version 7, GraphPad Software Inc., CA, USA). Descriptive statistics are given as mean and standard deviations if not indicated otherwise. For both modalities, the cortex/medulla ratio was calculated as signal (HU value) cortex/signal (HU) value medulla. Statistical significance was tested using a paired student's t-test. For simplification, the total kidney volume (TKV; representing the volume of both kidneys) was further analyzed as well as the percentage volume of the left kidney for SRF. For comparison between $RCV_{CT/MRI}$ and $MELV_{CT/MRI}$, Bland–Altman plots were calculated. The presented results include mean bias with standard deviation, 95% limits of agreement, and Pearson's correlations. The interobserver and intraobserver analyses were performed accordingly. P-values ≤ 0.05 were considered statistically significant.

Results

Study population and cortex/medulla ratio

Thirty two patients met the inclusion criteria. Three patients were excluded from further analysis due to incomplete coverage of the kidneys in the MRI datasets because the field-of-view was focused on the liver. Thus, the remaining 29 datasets (18 m/11 f; mean age: 62.8 $\pm$ 12.4 years, range 35–82 years) were used for further analyses (mean creatinine level: 0.96 $\pm$ 0.34 mg/dl; mean eGFR: 82.4 $\pm$ 22.1 ml/min/1.73 m^2). Besides renal cysts (BOSNIAK I), no kidney showed any substantial morphological pathology such as tumor or scar tissue. No renal artery stenoses were found. In all patients, RCV and MELV were obtained successfully using both imaging modalities. The mean cortex/medulla ratio was significantly ($p < 0.001$) higher as assessed on the CT datasets (3.5) compared to the MRI (2.5).

Intermodal comparison of RCV (RCV_{CT} vs. RCV_{MRI}): TKV and SRF

For RCV_{CT}, the difference between the mean values of TKV for reader 1 (R1) and reader 2 (R2) was 6.5%, with a difference between the corresponding mean values of SRF being 0.4%. For RCV_{MRI}, the difference between the mean values of TKV for R1 and R2 was 12.9% and that between the mean values of SRF 0.6%. The comparison of both modalities using Bland–Altman analysis revealed low mean biases of 0.6 $\pm$ 2.2% (R1) and -0.2 $\pm$ 2.0% (R2) with a 95% confidence interval (95% CI) of $-$ 0.2 to 1.4% and $-$ 0.1 to 0.5%, respectively. Pearson's correlation showed significant, high correlation coefficients of 0.73 (R1) and 0.79 (R2). Further results are given in Tables 1 and 2. The corresponding Bland–Altman plots are presented in Fig. 2a–e.

Intermodal comparison of MELV ($MELV_{CT}$ vs. $MELV_{MRI}$): TKV and SRF

For $MELV_{CT}$, the difference in the mean values of TKV for R1 and R2 was 10.1% and for the corresponding mean values of SRF 0.8%. For $MELV_{MRI}$, the difference between the mean values of TKV for R1 and R2 was 5.8% and that for the mean values SRF, the difference was 0.8%. Bland–Altman analysis showed very low mean biases of 0.1 $\pm$ 3.9% (R1) and 0.1 $\pm$ 4.8% (R2) with a 95% CI of

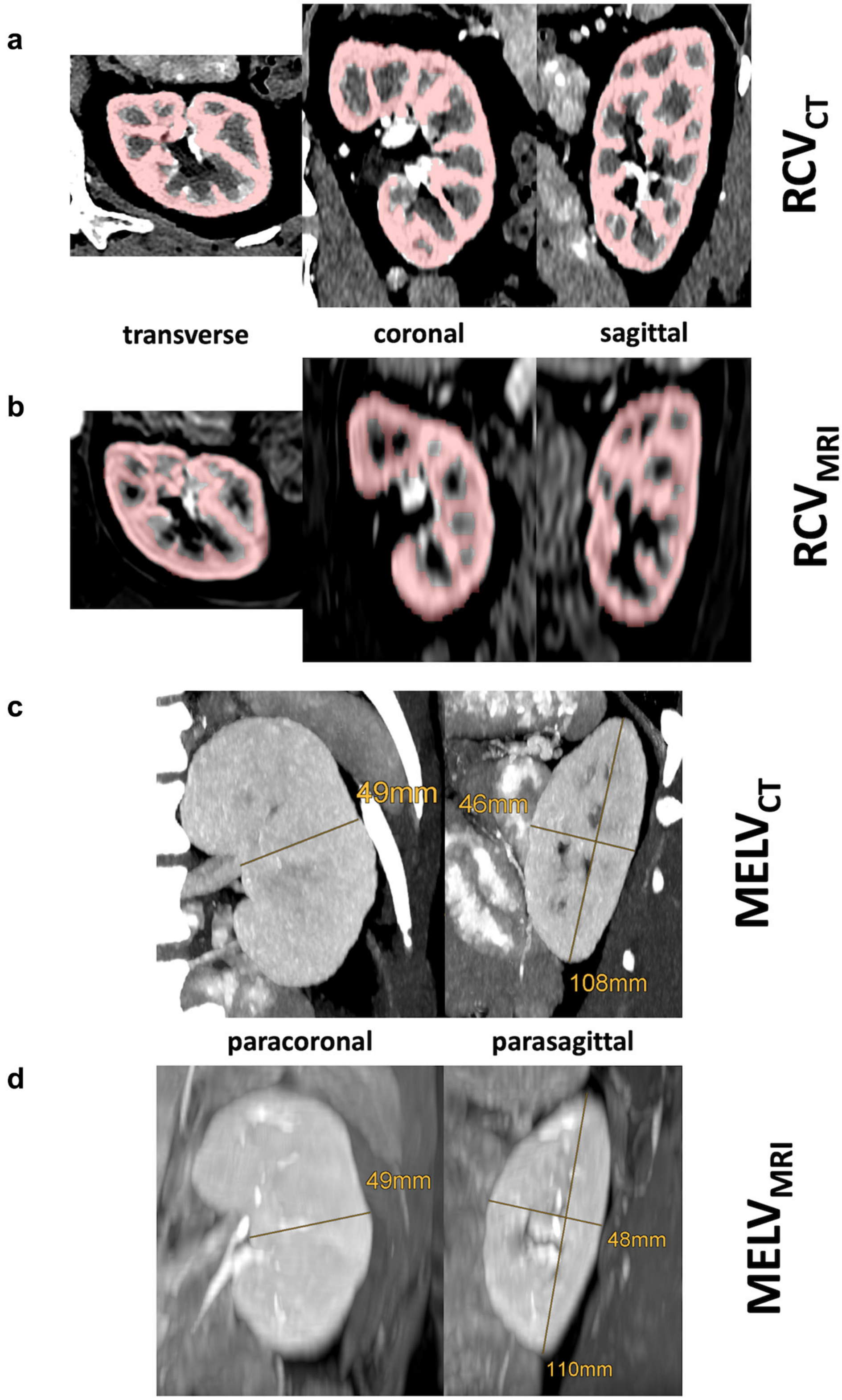

Fig. 1 Examples illustrating semiautomated registration of RCV and MELV using CT and MRI in the same patient. In RCV measurements (**a**, **b**), the cortex is delineated on arterial-phase CT and MR images using the Intellispace Platform (ISP 9.0, Philips Healthcare). The volume is calculated automatically. For MELV measurements (**c**, **d**), maximum intensity projections (MIPs) with a thickness of 3 cm from venous-phase CT and MRI images are generated in the individual adjusted orientation using a clinical DICOM viewer (IMPAX EE, AGFA Healthcare). Length and width are measured on paracoronal MIPs and thickness in the parasagittal plane. Total kidney volume is calculated using the modified ellipsoid formula

− 0.8 to 1.5% and − 1.1 to 1.8%, respectively. Pearson's correlation revealed a moderately significant correlation coefficient for R1 of 0.67 and a nonsignificant lower correlation for R2 of 0.45. Further results are given in Tables 1 and 2. The corresponding Bland–Altman plots are presented in Fig. 2c–g.

Table 1 Results of each individual volumetric method for assessment of total kidney volume, volumes of the right and left kidney, and percentage volume of the left kidney (estimated SRF)

Method		Kidney volume ± SD (cc)			SRF ± SD (%)
		Total	Right	Left	
RCV_{CT}	Reader 1	219.7 ± 42.9	109.7 ± 22.8	110.0 ± 21.8	49.9 ± 2.8
	Reader 2	205.5 ± 35.8	102.0 ± 19.8	103.5 ± 18.3	49.5 ± 3.0
	Δ (%)	14.2 (6.5)	7.7 (7)	6.5 (5.9)	0.4
RCV_{MRI}	Reader 1	233.2 ± 51.1	114.8 ± 26.2	118.3 ± 26.9	49.2 ± 3.0
	Reader 2	203.2 ± 32.3	101.2 ± 17.5	102.0 ± 17.4	49.8 ± 3.3
	Δ (%)	30.0 (12.9)	13.6 (11.9)	16.3 (13.8)	0.6
$MELV_{CT}$	Reader 1	309.7 ± 60.5	155.8 ± 39.3	153.9 ± 28.1	50.0 ± 5.0
	Reader 2	278.3 ± 62.0	137.2 ± 34.5	141.1 ± 32.8	49.2 ± 5.0
	Δ (%)	31.4 (10.1)	18.6 (11.9)	12.8 (8.3)	0.8
$MELV_{MRI}$	Reader 1	306.1 ± 54.2	153.8 ± 35.0	152.3 ± 24.6	49.9 ± 4.5
	Reader 2	288.3 ± 59.6	142.0 ± 34.2	146.3 ± 29.4	49.1 ± 4.0
	Δ (%)	17.8 (5.8)	11.8 (7.7)	6 (3.9)	0.8

For all volumes as well as for estimated SRF, the absolute (Δ) and percentage (%) differences between reader 1 and 2 are stated accordingly

Table 2 Comparison of estimated split renal function (SRF) for readers 1 and 2 including intra- and intermodal evaluations as well as interreader and intrareader agreement using Bland–Altman analysis, two-tailed Student's *t*-test, and Pearson's correlation assuming statistical significance for $p \leq 0.05$

Comparison of SRF (%)

Method	Mean bias	SD	95% CI	*p*-value	Correlation	*p*-value
Reader 1						
RCV_{CT} versus RCV_{MRI}	0.6	2.2	− 0.2 to 1.4	0.13	0.73	≤ 0.0001
$MELV_{CT}$ versus $MELV_{MRI}$	0.1	3.9	− 0.8 to 1.5	0.92	0.67	≤ 0.0001
RCV_{CT} versus $MELV_{CT}$	− 0.1	4.2	− 0.9 to 1.4	0.90	0.55	0.002
RCV_{MRI} versus $MELV_{MRI}$	− 0.6	4.3	− 1.0 to 0.9	0.42	0.41	0.003
Reader 2						
RCV_{CT} versus RCV_{MRI}	− 0.2	2.0	− 0.1 to 0.5	0.53	0.79	≤ 0.0001
$MELV_{CT}$ versus $MELV_{MRI}$	0.1	4.8	− 1.1 to 1.8	0.93	0.45	0.014
RCV_{CT} versus $MELV_{CT}$	0.4	5.0	− 1.2 to 2.2	0.70	0.29	0.13
RCV_{MRI} versus $MELV_{MRI}$	0.7	3.4	− 0.6 to 1.9	0.29	0.57	0.0013

Comparison of SRF (%)

Method	Mean bias	SD	95% LoA	*p*-value	Correlation	*p*-value
Interreader						
RCV_{CT}	0.7	2.8	− 4.9 to 6.2	0.23	0.89	≤ 0.0001
RCV_{MRI}	− 1.1	5.0	− 10.8 to 8.7	0.26	0.69	≤ 0.0001
$MELV_{CT}$	1.6	9.8	− 17.6 to 20.7	0.39	0.54	0.0013
$MELV_{MRI}$	− 1.5	8.6	− 18.5 to 15.4	0.33	0.50	0.006
Intrareader						
RCV_{CT}	− 1.2	2.1	− 5.3 to 3.0	0.12	0.92	≤ 0.001
RCV_{MRI}	− 1.1	1.3	− 3.7 to 1.4	0.02	0.97	≤ 0.0001
$MELV_{CT}$	1.5	4.9	− 8.0 to 11.0	0.29	0.88	≤ 0.001
$MELV_{MRI}$	6.2	8.7	− 10.9 to 23.3	0.04	0.64	0.047

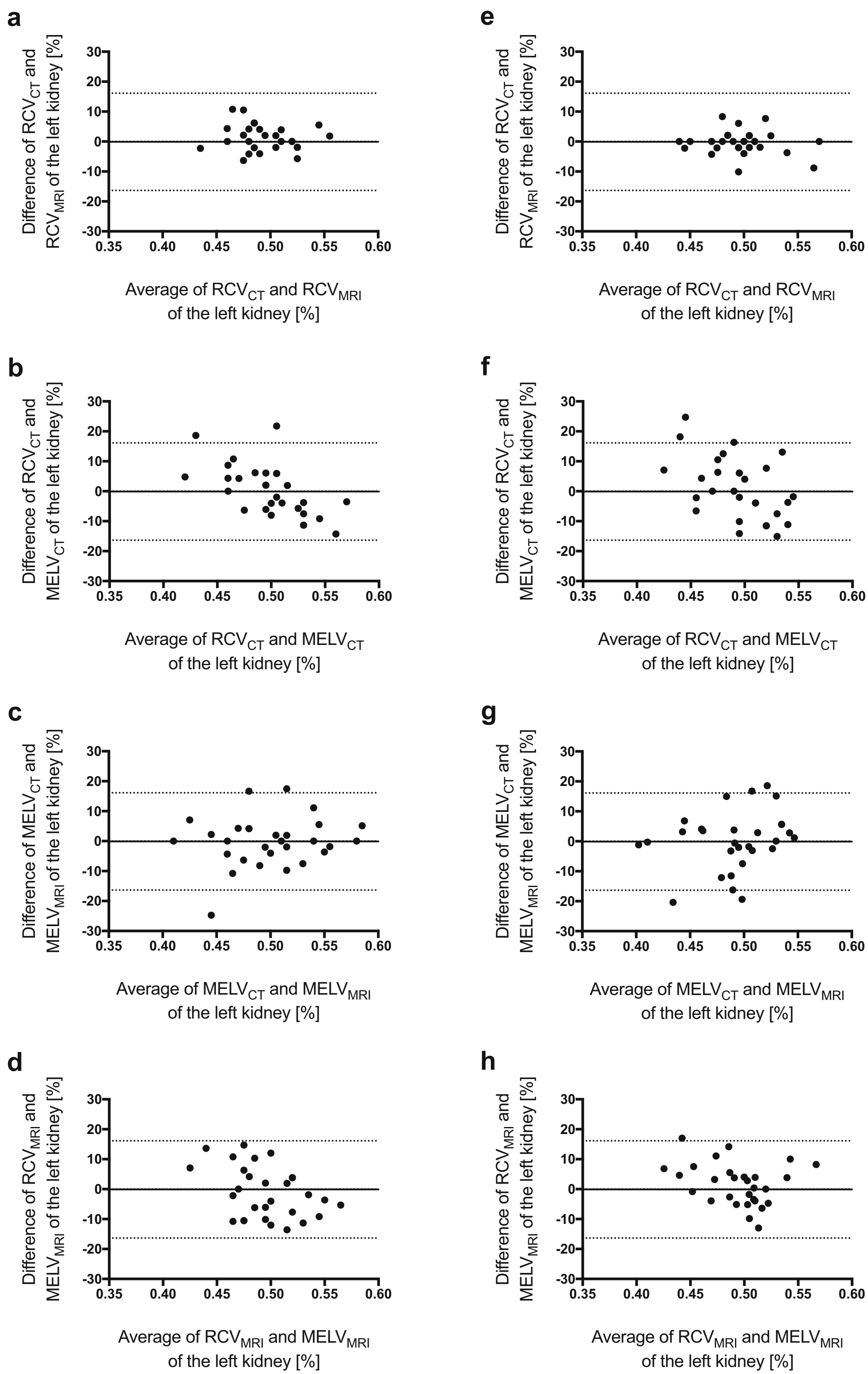

Fig. 2 Bland–Altman plots representing SRF calculated by *reader 1* (**a**–**d**) and *reader 2* (**e**–**h**). Results show excellent agreement between RCV_{CT} and RCV_{MRI} with MELV showing substantially higher variability

Intramodal method-comparison (RCV_{CT} vs. $MELV_{CT}$ and RCV_{MRI} vs. $MELV_{MRI}$): SRF

For RCV_{CT} and $MELV_{CT}$, the mean SRF is almost identical with a difference of 0.1% (R1) and 0.3% (R2). Bland–Altman analysis showed low mean biases of − 0.1 ± 4.2% (R1) and 0.4 ± 5.0% (R2) with a 95% CI of − 0.9 to 1.4% and − 1.2 to 2.2%, respectively. Pearson's correlation showed a moderately significant correlation coefficient for R1 of 0.55 and a nonsignificant low correlation for R2 of 0.29. Further results are given in Tables 1 and 2. The corresponding Bland–Altman plots are presented in Fig. 2b–f.

For RCV_{MRI} and $MELV_{MRI}$, the mean SRF is slightly higher than that for CT but still acceptable with a difference of 0.7% for both readers. Bland–Altman analysis showed moderate mean biases of − 0.6 ± 4.3% (R1) and 0.7 ± 3.4% (R2) with a 95% CI of − 1.0 to 0.9% and − 0.6 to 1.9%, respectively. Pearson's correlation revealed a low correlation coefficient for R1 of 0.41 and a moderately significant correlation for R2 of 0.57. Further results are given in Tables 1 and 2. The corresponding Bland–Altman plots are presented in Fig. 2d–h.

Interreader agreement analysis

The interreader agreement was strong for RCV_{CT} with a statistically significant Pearson's correlation coefficient of 0.89. The mean bias between the readers was 0.7 ± 2.8% with 95% limits of agreement (95% LoA) of − 4.9% to 6.2%. RCV_{MRI} had a good agreement with a significant Pearson's correlation of 0.69 with a mean bias of − 1.1 ± 5.0% and 95% LoA of − 10.8 to 8.7%. $MELV_{CT}$ and $MELV_{MRI}$ showed only moderately significant correlations of 0.54 and 0.5, respectively, with a mean bias of 1.6 ± 9.8% ($MELV_{CT}$)/− 1.5 ± 8.6% ($MELV_{MRI}$) with 95% LoA of − 17.6 to 20.7% ($MELV_{CT}$)/− 18.5% to 15.4% ($MELV_{MRI}$). The results are summarized in Table 2 with the corresponding Bland–Altman plots shown in Fig. 3.

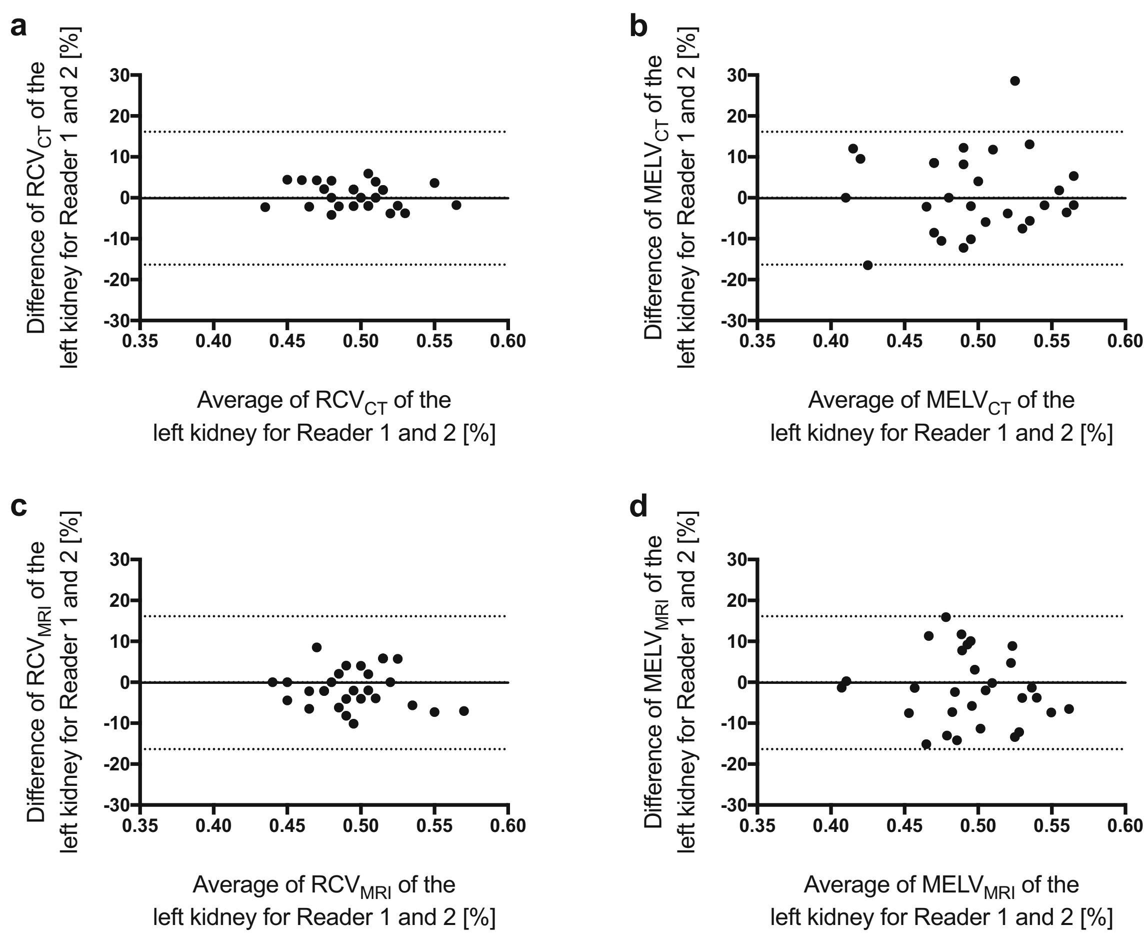

Fig. 3 Bland–Altman plots representing interreader agreement. The greatest interreader agreement was obtained with RCV_{CT} (**a**). MELV method (**b**, **d**) has a wider spread of results compared with RCV method (**a**, **c**)

Intrareader agreement analysis

Using the RCV method, the intrareader agreement was excellent for RCV_{CT} as well as RCV_{MRI} with statistically significant Pearson's correlation coefficients of 0.92 and 0.97, respectively. For RCV_{CT}, the mean bias between the repeated measurements was − 1.2 ± 2.8% with 95% LoA of − 5.3 to 3.0%. For RCV_{MRI}, the mean bias was − 1.1 ± 1.3% with 95% LoA of − 3.7 to 1.4%. The MELV method showed excellent agreement only for $MELV_{CT}$ with moderate agreement for $MELV_{MRI}$ with statistically significant Pearson's correlation coefficients of 0.88 and 0.64, respectively. For $MELV_{CT}$, moderate mean was 1.5 ± 4.9% with 95% LoA of − 8.0 to 11%. $MELV_{MRI}$ had a high mean bias of 6.2 ± 8.7% with 95% LoA of − 10.9 to 23.3%. The results are summarized in Table 2 with corresponding Bland–Altman plots shown in Fig. 4.

Discussion

This study aimed to evaluate on an interindividual and intraindividual basis the comparison of SRF measurements between contrast-enhanced MRI and CT using two different volumetric approaches. The two evaluated methods were RCV and MELV, which are well established and used clinically. RCV demonstrated superior results with higher precision for both CT and MRI compared to MELV. Comparison of RCV_{CT} and RCV_{MRI} revealed a high level of agreement regarding inter and intrareader reliability and RCV_{CT} showed better results, followed by RCV_{MRI}.

Regarding TKV, the current results using RCV_{CT} are comparable to those in the literature [4, 5, 8, 16]. Nevertheless, the renal cortex volumes in the literature vary depending on the subjects included (healthy volunteers vs. patients with known kidney disease). Thus, a direct comparison of literature results and our findings is limited. The study by Halleck et al. [4] was one of the first to analyze the potential of RCV for preoperative evaluation of renal function in living kidney donors with similar results to our

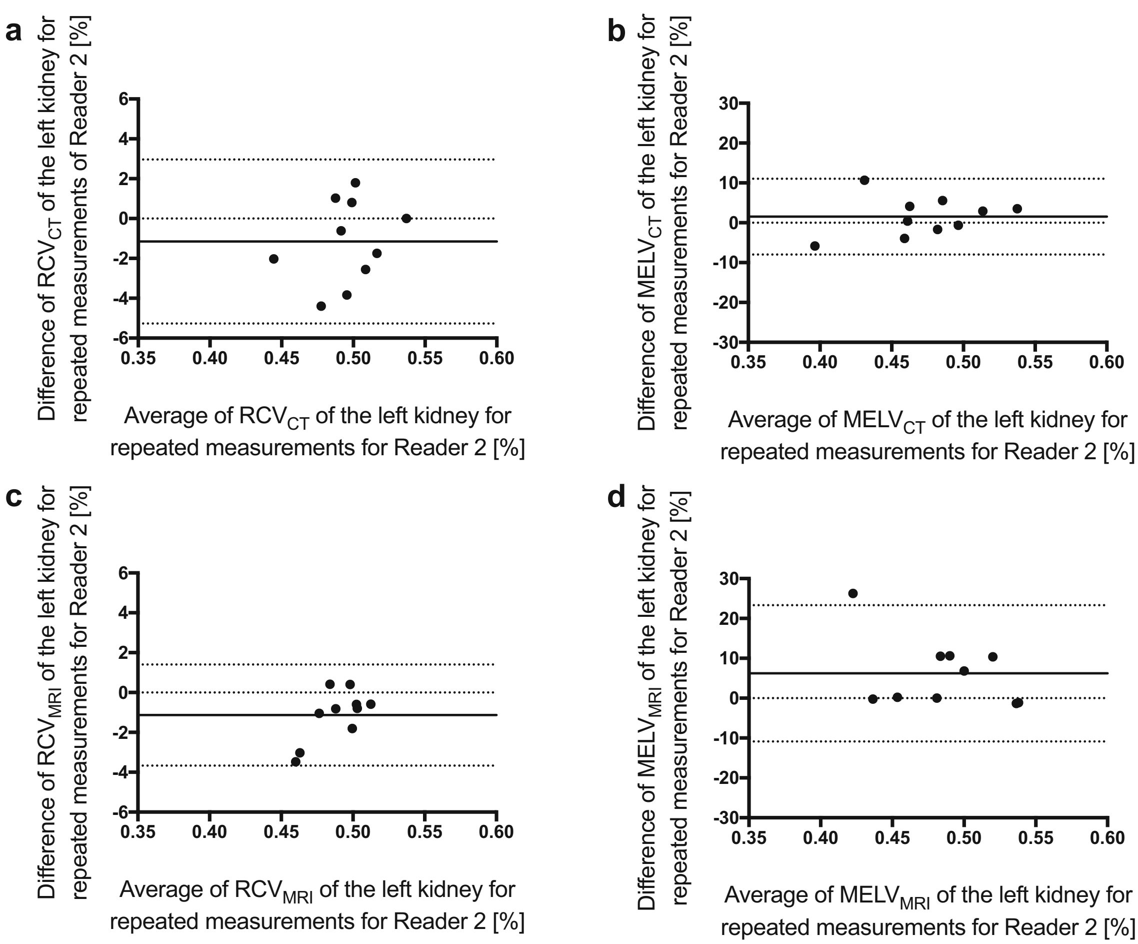

Fig. 4 Bland–Altman plots representing the intrareader agreement. The greatest intrareader agreement was obtained with RCV_{CT} (**a**). The MELV method (**b**, **d**) has a wider spread of results compared with the RCV method (**a**, **c**)

study. Wahba et al. [5] evaluated RCV and MELV among other parameters to measure SRF in CT datasets. For RCV_{CT} they calculated a slightly lower mean TKV in 101 living kidney donors. Shimoyama et al. [15] compared renal volumetry methods including RCV and MELV in 32 patients undergoing radical nephrectomy. Presumably due to the preexisting kidney diseases such as renal cell carcinoma, the mean kidney volume was substantially lower (≈ 1/3) in those studies than the current results. There is only one publication referring to the assessment of renal cortex volume using MR images. Will et al. [16] investigated an automated segmentation algorithm using non-contrast enhanced T1- and T2- weighted images. Their results are similar to the results of reader 1 but differ from the results of reader 2 by 19.4%. To date, there are no intraindividual data comparing RCV values obtained on CT versus MRI.

The measured kidney volumes for MELV are greater compared to RCV because the latter method only includes the renal cortex. Our results for the total kidney volume (TKV) using $MELV_{CT}$ revealed a statistically significant difference of about 10.1% between R1 (309.7 ± 60.5 cc) and R2 (278.3 ± 62.0 cc). The results of reader 1 are more congruent with the published data for healthy renal donors [5]. One possible explanation for the interreader differences could be the difficulty of standardization of the MELV method. The degrees of freedom to choose the appropriate angulation in three planes for a MIP dataset are manifold. This source of error is crucial, because small deviations in angulation can lead to a significant difference in renal volume. Nevertheless, in interreader evaluation of the SRF, the effect on the mean SRF was minimal.

In the literature, only a few publications have described the measurement of the TKV using MELV in MRI datasets. The interpretation of our results in the context of the existing literature is difficult due to different technical parameters, including field strength, utilized sequences and spatial resolution. Seuss et al. [8] evaluated $MELV_{MRI}$ using noncontrast-enhanced T2-weighted MR images in 24 healthy volunteers achieving a slightly higher mean TKV. While the results of TKV published by Cheong et al. [17] are lower, they validated $MELV_{MRI}$ using ex vivo and in vivo models and established a normal range of values for each kidney ranging from 132 to 276 cc in men and 87 to 223 cc in women.

In terms of interreader agreement, RCV_{CT} showed the highest reproducibility (Pearson's correlation: 0.89), RCV_{MRI} showed reliable results (0.69), but $MELV_{CT}$ (0.54) and $MELV_{MRI}$ (0.50) showed only moderate interreader agreement. Publications analyzing interreader agreement are sparse for CT and not available for MRI. Soga et al. [6] showed an excellent interobserver agreement for MELV in CT datasets with a low bias of -0.1% and limits of agreement of − 5.1% to 5.3%. Seuss et al. [8] found no significant difference (− 0.2 ml) in comparisons of the results from three different readers with an average error of 6.4 ml.

The reason for improved interreader agreement with CT compared to MRI datasets is probably the higher spatial resolution of CT compared to MRI which enables superior depiction of kidney margins and adjacent vessels, particularly in the hilum and renal pelvis. In particular, for RCV the labeling of the cortex along its margin on every slice is important to achieve an exact result. In comparison, the possibility for individual adjustments is much higher for MELV than for RCV measurements. Especially for MELV, the alignment of the kidney along its true axis as well as the measurement of the width of the kidney using vague landmarks at the level of the hilus and pelvis [8] fosters interindividual differences in volume measurements, reducing interindividual comparability.

Intrareader agreement was high for RCV_{CT} (0.92) as well as RCV_{MRI} (0.97) in the current study. $MELV_{CT}$ showed higher agreement than $MELV_{MRI}$ (0.88/0.64). The aforementioned study by Seuss et al. [8] found no significant difference (− 0.4 ml) for repeated measurements by the same reader with an average error of 5.2 ml. The other previously mentioned publications did not determine intrareader agreement.

From the perspective of volume determination of both kidneys (TKV), the differences between CT and MRI are distinct. However, the percentage volume differences between both kidneys for calculating SRF are far more relevant than the corresponding absolute values. When mean SRF measured using RCV was compared for both modalities in our group of patients, the results were similar. Interreader analysis also revealed a comparable mean bias for RCV_{MRI} but a higher range of values in total of 19.5% compared to RCV_{CT} (range 11.1%). Intrareader analysis showed comparable results between both modalities with a similar range of values (RCV_{CT}: 8.3%; RCV_{MRI}: 5.1%). The mean SRF measured using MELV was almost identical between CT and MRI in our group of patients. Interreader analysis revealed a comparable moderate mean bias for both modalities with higher standard deviations compared to RCV method. More importantly, MELV method revealed a much higher range of values compared to RCV method, in total 38.3% ($MELV_{CT}$) and 33.9% ($MELV_{MRI}$). Furthermore, intrareader analysis resulted in much higher mean bias and range of values for $MELV_{MRI}$ (bias: 6.2 ± 8.7%; range 34.2%) compared to $MELV_{CT}$ (bias: 1.5 ± 4.9%; range 19%). If MELV method, especially when performed on MRI datasets, is used for the determination of the SRF before LKD, the responsible surgeon should be aware of these drawbacks, particularly the possible higher range of values. If the responsible surgeon is certain that the lower accuracy and reliability of MELV method is clinically acceptable without risk to the donor's future kidney function and associated complications, MELV method could be utilized for estimation of SRF.

Beyond the comparison of the volumetric approaches, some general considerations for both MRI and CT should be mentioned. Both imaging modalities are difficult to completely standardize in clinical routine, especially MRI. The lack of standardization is multifactorial ranging from different technical capabilities of scanners, different protocols at different sites as well as different vendors, and differences in timing of the contrast bolus. Both volumetric approaches used in our study are dependent upon the administered contrast agent accentuating differences between the renal cortex and the renal medulla. Consequently, optimal enhancement of the cortex is crucial for the determination of the RCV with CT as well as MRI. Despite a multiphase protocol with several fixed contrast phases being used at our institution for contrast-enhanced MRI (after visual bolus triggering), CT datasets (with a fixed delay after HU-based bolus-triggering) seemed to be more robust. A further intrinsic advantage of CT is that the differential enhancement between the renal cortex and medulla in the arterial phase appears more pronounced than that obtained with Gadolinium based contrast agents. Further technical differences between both imaging modalities include the required breath-hold, which is longer with MRI ($\sim$ 15 s) compared to CT ($\sim$ 7 s), thus leading to a generally more robust image quality in the upper abdomen for CT. A further technical topic, which should be addressed, is the spatial resolution of both modalities. In this study, both CE-CT and CE-MRI datasets could be analyzed with 2 mm slice thickness, enabling comparison of both (RCV vs. MELV) measurement methods. However, in clinical routine, slice thickness with MRI is often greater, a factor which should be considered if implementing volumetric MRI for the workup of kidney donors.

Some limitations should be discussed in the context of this study. (1) First, our sample size is limited due to the strict inclusion criterion requiring patients to have received CT and MRI within 3 months of one another. (2) This study aimed only to compare the two imaging modalities with respect to the two assessed volumetric methods. The question as to which technique is most appropriate from a clinical perspective is beyond the scope of this work but has been addressed elsewhere in the literature (e.g., [5]). (3) Although TKV has shown to correlate significantly with gender [17], this technical study assessed purely volume determinations. (4) Our inter- and intrareader analysis was performed by an experienced reader with board certification and a resident, formally a less-experienced reader.

Conclusion

Modern volumetric imaging tools, such as RCV or MELV, allow for the evaluation of SRF necessary for living kidney donor (LKD) assessment using common contrast-enhanced CT or MR images. Kidney volumetry in determining SRF is as accurate and reliable with CE-MRI as with CE-CT datasets with regard to RCV method; however, MELV method shows generally lower accuracy and reliability, particularly with CE-MRI. RCV_{CT} was superior to RCV_{MRI} with respect to intra- and interobserver variability. However, when healthy donors are to be evaluated for possible LKD, MRI is relatively advantageous to CT due to the lack of ionizing radiation exposure. Thus, CT of healthy donors should only be undertaken if the benefits outweigh this drawback. Nevertheless, the decision as to the appropriate modality must be chosen according to individual circumstances.

Funding This research did not receive any specific grant from funding agencies in the public, commercial, or not-for-profit sectors.

Compliance with ethical standards

Conflict of interest All authors approve publication of our work and have no conflict of interest.

Ethical approval All procedures performed in studies involving human participants were in accordance with the ethical standards of the institutional and/or national research committee and with the 1964 Helsinki declaration and its later amendments or comparable ethical standards. For this type of study formal consent is not required.

References

1. Ibrahim HN, Foley R, Tan L, et al. (2009) Long-term consequences of kidney donation. N Engl J Med 360:459–469. https://doi.org/10.1056/NEJMoa0804883
2. Terasaki PI, Cecka JM, Gjertson DW, Takemoto S (1995) High Survival Rates of Kidney Transplants from Spousal and Living Unrelated Donors. N Engl J Med 333:333–336. https://doi.org/10.1056/NEJM199508103330601
3. Wolfe RA, Ashby VB, Milford EL, et al. (1999) Comparison of mortality in all patients on dialysis, patients on dialysis awaiting transplantation, and recipients of a first cadaveric transplant. N Engl J Med 341:1725–1730. https://doi.org/10.1056/NEJM199912023412303
4. Halleck F, Diederichs G, Koehlitz T, et al. (2013) Volume matters: cT-based renal cortex volume measurement in the evaluation of living kidney donors. Transpl Int 26:1208–1216. https://doi.org/10.1111/tri.12195
5. Wahba R, Franke M, Hellmich M, et al. (2016) Computed Tomography Volumetry in Preoperative Living Kidney Donor Assessment for Prediction of Split Renal Function. Transplantation 100:1270–1277. https://doi.org/10.1097/TP.0000000000000889

6. Soga S, Britz-Cunningham S, Kumamaru KK, et al. (2012) Comprehensive comparative study of computed tomography-based estimates of split renal function for potential renal donors: modified ellipsoid method and other CT-based methods. J Comput Assist Tomogr 36:323–329. https://doi.org/10.1097/RCT.0b013e318251db15
7. Kato F, Kamishima T, Morita K, et al. (2011) Rapid estimation of split renal function in kidney donors using software developed for computed tomographic renal volumetry. Eur J Radiol 79:15–20. https://doi.org/10.1016/j.ejrad.2009.11.013
8. Seuss H, Janka R, Prümmer M, et al. (2017) Development and Evaluation of a Semi-automated Segmentation Tool and a Modified Ellipsoid Formula for Volumetric Analysis of the Kidney in Non-contrast T2-Weighted MR Images. J Digit Imaging 30:244–254. https://doi.org/10.1007/s10278-016-9936-3
9. Gardan E, Jacquemont L, Perret C, et al. (2018) Renal cortical volume: high correlation with pre- and post-operative renal function in living kidney donors. Eur J Radiol 99:118–123. https://doi.org/10.1016/j.ejrad.2017.12.013
10. Hyodoh H, Shirase R, Kawaharada N, et al. (2009) MR angiography for detecting the artery of Adamkiewicz and its branching level from the aorta. Magn Reson Med Sci 8:159–164. https://doi.org/10.2463/mrms.8.159
11. Schneider G, Massmann A, Altmeyer K, Katoh M, Bücker A (2007) MR imaging and MR angiography of the aorta. Radiologe 47:993–1002. https://doi.org/10.1007/s00117-007-1582-9
12. Karlo C, Reiner CS, Stolzmann P, et al. (2010) CT- and MRI-based volumetry of resected liver specimen: comparison to intraoperative volume and weight measurements and calculation of conversion factors. Eur J Radiol 75:e107–e111. https://doi.org/10.1016/j.ejrad.2009.09.005
13. Lee J, Kim KW, Kim SY, et al. (2014) Feasibility of semiautomated MR volumetry using gadoxetic acid-enhanced MRI at hepatobiliary phase for living liver donors. Magn Reson Med 72:640–645. https://doi.org/10.1002/mrm.24964
14. Huynh HT, Karademir I, Oto A, Suzuki K (2014) Computerized liver volumetry on MRI by using 3D geodesic active contour segmentation. Am J Roentgenol 202:152–159. https://doi.org/10.2214/AJR.13.10812
15. Shimoyama H, Isotani S, China T, et al. (2017) Automated renal cortical volume measurement for assessment of renal function in patients undergoing radical nephrectomy. Clin Exp Nephrol 21:1124–1130. https://doi.org/10.1007/s10157-017-1404-y
16. Will S, Martirosian P, Würslin C, Schick F (2014) Automated segmentation and volumetric analysis of renal cortex, medulla, and pelvis based on non-contrast-enhanced T1- and T2-weighted MR images. MAGMA 27:445–454. https://doi.org/10.1007/s10334-014-0429-4
17. Cheong B, Muthupillai R, Rubin MF, Flamm SD (2007) Normal values for renal length and volume as measured by magnetic resonance imaging. Clin J Am Soc Nephrol 2:38–45. https://doi.org/10.2215/CJN.00930306